Organic solar cells with solution-processed graphene transparent electrodes

Junbo Wu,[1] Héctor A. Becerril,[2] Zhenan Bao,[2] Zunfeng Liu,[3] Yongsheng Chen,[3] and Peter Peumans[4,a]

[1]*Department of Materials Science and Engineering, Stanford University, Stanford, California 94305, USA*
[2]*Department of Chemical Engineering, Stanford University, Stanford, California 94305, USA*
[3]*Key Laboratory for Functional Polymer Materials and Center for Nanoscale Science and Technology, College of Chemistry, Institute of Polymer Chemistry, Nankai University, Tianjin 300071, People's Republic of China*
[4]*Department of Electrical Engineering, Stanford University, Stanford, California 94305, USA*

We demonstrate that solution-processed graphene thin films can serve as transparent conductive anodes for organic photovoltaic cells. The graphene electrodes were deposited on quartz substrates by spin coating of an aqueous dispersion of functionalized graphene, followed by a reduction process to reduce the sheet resistance. Small molecular weight organic solar cells can be directly deposited on such graphene anodes. The short-circuit current and fill factor of these devices on graphene are lower than those of control device on indium tin oxide due to the higher sheet resistance of the graphene films. We anticipate that further optimization of the reduction conditions will improve the performance of these graphene anodes. © *2008 American Institute of Physics.*
[DOI: 10.1063/1.2924771]

Organic optoelectronic devices such as organic photovoltaic (OPV) cells,[1,2] organic light-emitting diodes,[3,4] and organic photodetectors[5,6] have attracted interest because they can be deposited on flexible, light-weight substrates using low-cost fabrication methods. An important aspect of optoelectronic thin-film devices is the transparent, conductive electrode through which light couples in or out of the devices. Indium tin oxide (ITO) is widely used but may be too expensive[7] for an application such as solar cells. Moreover, metal oxides such as ITO are brittle and therefore of limited use on flexible substrates.[8] A substitute for ITO with a similar performance but lower cost is clearly needed. Recent work on solution-processed random meshes of carbon nanotubes[9–11] and metal nanowires[12,13] has resulted in solution-processed, conductive, transparent electrodes with transparencies and sheet resistances that approach or exceed that of ITO. However, the electrodes realized using the above approaches have a roughness that is comparable with or larger than a typical device thickness, leading to frequent shorts.

The two-dimensional conductor graphene is a promising transparent conductor because of its optical and electrical properties.[14–16] In principle, electrons in individual graphene sheets delocalize over the complete sheet, which provide ballistic charge transport in a one-atom-thick material with very little optical absorption. In practice, however, large-area graphene films produced via solution processing of functionalized graphene contain multiple grain boundaries and incorporate lattice defects and oxidative traps that increase the electrical resistance of the material. As a result, the films must be made thicker than one atomic layer to obtain practical sheet resistances. Recently, such graphene thin films were used as an anode in dye-sensitized solar cells.[17] In this letter, we demonstrate that very thin films of graphene can be used as anode in solid-state thin-film OPV cells with a performance that approaches that of ITO while not exhibiting

the roughness problems of carbon nanotube or metal nanowire meshes. The trade-off between transparency and sheet resistance is also investigated.

Various methods to make thin films of graphene have been developed such as the scotch tape method[14] and epitaxial growth,[18] but these methods are not suitable for low-cost, large-area optoelectronics. The graphene electrodes used in this work were deposited on quartz slides by spin-coating dispersions of functionalized graphene in water. The functionalized graphene material was prepared through a modified Hummers method[19,20] as described elsewhere.[21] Briefly, a graphite crystal was chemically oxidized by treatment with various solutions of $NaNO_3$, $KMnO_4$, concentrated H_2SO_4, and 30 wt % H_2O_2, washed with HCl and purified water, and ultrasonicated to exfoliate individual graphene oxide sheets. This procedure produces a loose brown powder that can be dispersed in water at loadings of up to $\sim$15 mg/ml. The spin-coating rate was increased every 30 s from an initial value of 500–800 rpm to gradually spread the water dispersion on the quartz, and finally to 1600 rpm to dry the film. Residual water was removed by heating these films to 100 °C in a vacuum oven for several hours.

The resulting functionalized graphene films are not conductive and the material must be reduced to obtain acceptable sheet resistances. The reduction process removes oxidized functionalities from the film and partially restores electron delocalization, which increases both the light absorption and electrical conductivity of the film. The effectiveness of the reduction of functionalized graphene films by chemical and thermal methods has been characterized[17,21] with chemical treatments being less effective than thermal procedures. The dependence of optical and electrical properties of reduced graphene films on the reduction process are discussed elsewhere.[21] In this work, the graphene films were reduced either by vacuum annealing at 1100 °C or by a combination of a hydrazine treatment and Ar annealing at 400 °C.
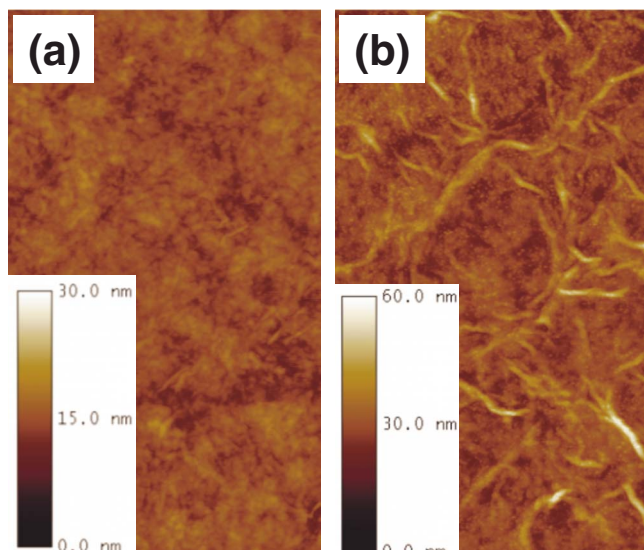
[a]Electronic mail: ppeumans@stanford.edu.

FIG. 1. (Color online) AFM images of reduced (a) thin (<10 nm) and (b) thick (>10 nm) graphene films. The scan size is 3 μm in (a) and 8 μm in (b).

FIG. 3. (Color online) Transmittance as a function of wavelength for graphene films of various thicknesses. The graphene films were reduced by the hydrazine treatment and argon annealing at 400 °C.

Figure 1(a) shows a typical atomic force microscopy (AFM) image of a graphene film after reduction using a hydrazine treatment and Ar annealing with a thickness of <10 nm. The surface of the film presents some corrugations that possibly arise from partial roll up of the edges of individual graphene sheets. The root mean surface roughness is $R_q \sim 3$ nm. Figure 1(b) shows the morphology of a thicker graphene film (>10 nm) exhibiting extended wrinkles leading to $R_q \sim 9$ nm. In both cases, the film surfaces are free from spikes which would lead to shorts in thin-film optoelectronic devices. The thick, spin-coated conductive polymer buffer layer that is used in devices with carbon nanotube or metal nanowire mesh transparent electrodes is therefore not necessary to prevent shorts when using these graphene electrodes. Since the film thicknesses exceed the thickness of a single layer of graphene, the films used here mostly consist of multiple layers of graphene.

Figure 2 shows the optical transmittance (triangles, measured at $\lambda=550$ nm) and sheet resistance (circles) versus thickness for graphene films reduced by either vacuum annealing (open symbols) or a combination of a hydrazine treatment and Ar annealing (closed symbols). The film thickness was measured by using AFM across edges and steps in the films. The sheet resistance was measured in a two-electrode configuration and includes the contact resistance between the graphene film and vapor-deposited gold electrodes used to probe the films. Both transmittance and sheet resistance decrease with increasing film thickness. Reduction by vacuum annealing produces graphene films with slightly better transparency and conductivity compared to the films reduced using the hydrazine treatment and Ar annealing. For the film thicknesses of <20 nm, the optical transmittance is generally $>80\%$, while the sheet resistance varies from 5 kΩ/sq to 1 MΩ/sq. The dependence of transmittance on wavelength is shown in Fig. 3 for three graphene films with different thicknesses, which were reduced by the hydrazine treatment and argon annealing. The optical transparency monotonically decreases for decreasing wavelengths over the spectral range $\lambda=400-1800$ nm.

The sheet resistance of the graphene films shown here is much higher than that of ITO films for the same transparency. This may be because the functionalized graphene is not completely reduced. Furthermore, since the average size of the sheets was 364 ± 120 nm measured along the longest axis, charge carriers have to hop between individual flakes. Finally, the films are not uniform and thinner regions of the film may act as bottlenecks that limit the overall in-plane conductivity.

Bilayer small molecule OPV cells were fabricated on graphene films on quartz and on commercially obtained 130-nm-thick ITO on glass (sheet resistance of <20 Ω/sq) as transparent anode. All organic materials were commercially obtained and then purified using thermal gradient sublimation.[22] The organic thin films and metal cathode were deposited at room temperature by thermal evaporation in high vacuum ($\sim 10^{-7}$ Torr). The layer structure of the devices is anode/copper phthalocyanine (CuPc)/fullerene (C_{60})/bathocuproine (BCP)/100 nm Ag. The Ag cathode was deposited through a shadow mask with circular openings of 0.81 mm^2. The current density-voltage (J-V) curves were measured at room temperature under 85 mW/cm^2 AM1.5G simulated solar illumination from a filtered 500 W Xe arc lamp. The illumination intensity was measured by using a calibrated silicon photodiode. No corrections were made for the spectral mismatch.
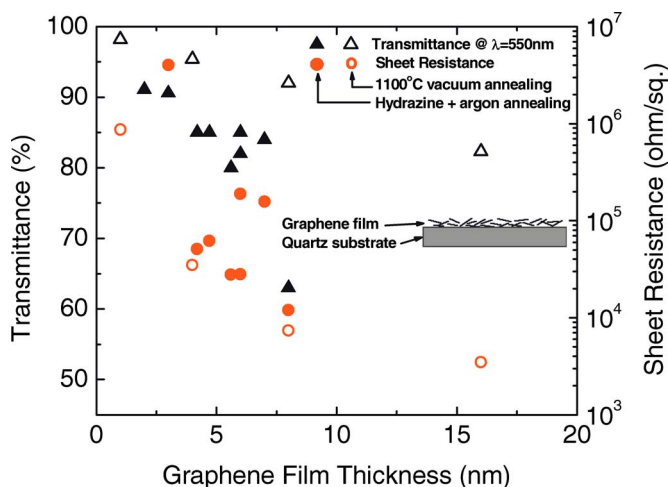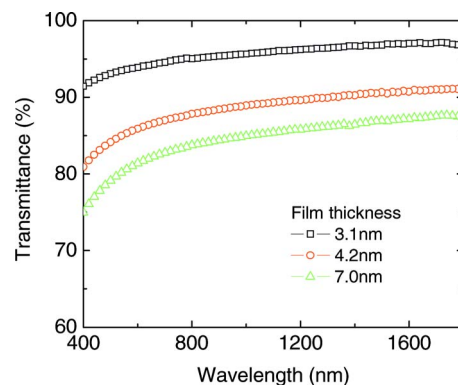

FIG. 2. (Color online) Transmittance at $\lambda=550$ nm (triangles) and sheet resistance (circles) as a function of the graphene film thickness for both reduction methods: vacuum annealing at 1100 °C (open symbols) and hydrazine treatment and argon annealing at 400 °C (filled symbols).
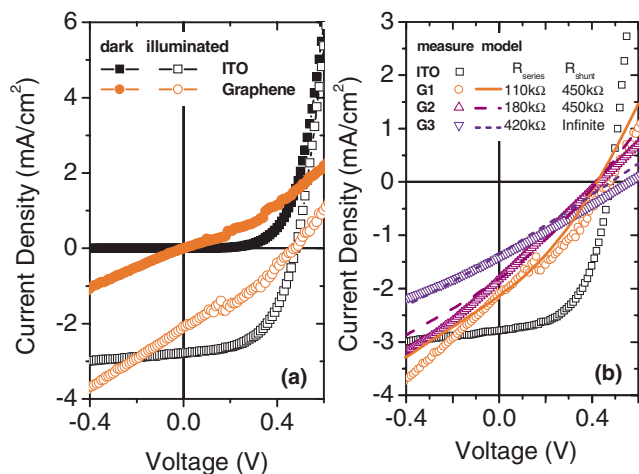
FIG. 4. (Color online) (a) Current density voltage (*J-V*) curves for an OPV cell with layer structure of 35 nm CuPc/50 nm C_{60}/10 nm BCP/100 nm Ag on graphene (circles) and ITO (squares) in the dark (filled symbols) and under 85 mW/cm^2 AM1.5G simulated solar illumination (open symbols). The sheet resistance and transmittance of the graphene film are ~100 kΩ/sq and 95%, respectively. (b) *J-V* curves for OPV cells on ITO (squares) and three different graphene films (circles, triangles, and inverted triangles) under AM1.5G simulated solar illumination. Using the data for the cell on ITO, the *J-V* curves of the cells on graphene are reproduced by adding a resistive voltage drop to the voltage axis (solid line, dashed line, and short dashed line) and a shunt resistance.

The thickness of graphene films used to fabricate OPV cells is between 4 and 7 nm, and the corresponding values of the transmittance and sheet resistance are 85%–95%, and 100 to 500 kΩ/sq, respectively. The *J-V* curves of a typical cell with layer structure of 35 nm CuPc/50 nm C_{60}/10 nm BCP on graphene and ITO are shown in Fig. 4(a), where the graphene film was reduced by vacuum annealing. The short-circuit current density J_{SC}, open circuit voltage V_{OC}, fill factor FF, and power conversion efficiency η are 2.1 mA/cm^2, 0.48 V, 0.34, and 0.4%, respectively, for the cell on graphene, and 2.8 mA/cm^2, 0.47 V, 0.54, and 0.84%, respectively, for the cell on ITO. The efficiency of the ITO control device is well below the best published data[23,24] for the material system used because the device structure and deposition conditions were not optimized. In spite of different work functions of graphene (4.4–4.65 eV)[25,26] and ITO (4.5–5.1 eV),[27–29] the difference in V_{OC} is <100 mV. This indicates that V_{OC} is determined by the difference between Fermi levels of the unintentionally doped donor (CuPc) and acceptor (C_{60}) materials.[30] The lower efficiency of the cell on graphene is mainly due to a reduced J_{SC} and FF compared to the cell on ITO, both of which are due to the high sheet resistance of the graphene film. Furthermore, a smaller shunt resistance is seen for devices on graphene electrodes, which leads to an increase in current in reverse bias, in the dark, and under illumination. Using experimental data for cells on ITO, *J-V* curves for the cells on graphene can be reproduced by including an extra voltage drop due to a series resistor to the voltage axis and (dark) leakage current due to a shunt resistance. As shown in Fig. 4(b), the modeled *J-V* curves match the experimental data of cells on graphene. The series resistances used to obtain these fits, $R_{1,series}$=110 kΩ, $R_{2,series}$=180 kΩ, and $R_{3,series}$=420 kΩ, are very close to the measured sheet resistances of the graphene films used: R_1=75–150 kΩ, R_2=200 kΩ, and R_3=200 kΩ–3 MΩ, respectively.

In conclusion, we demonstrated that solution-processed graphene films can be used as a transparent conductive electrode for OPV cells. For film thicknesses of <20 nm, the optical transmittance is >80%, while the sheet resistance varies from 5 kΩ/sq to 1 MΩ/sq. Compared to control devices on ITO, it was shown that the lower J_{SC} and FF of bilayer small molecular weight OPV cells are mainly caused by the high sheet resistance of the graphene thin films. Improved graphene film treatments will be required to improve the sheet resistance without compromising transmittance. In addition, processes need to be developed, which are compatible with low-cost flexible substrates.

[1]C. W. Tang, Appl. Phys. Lett. **48**, 183 (1986).
[2]P. Peumans, A. Yakimov, and S. R. Forrest, J. Appl. Phys. **93**, 3693 (2003).
[3]C. W. Tang and S. A. Van Slyke, Appl. Phys. Lett. **12**, 913 (1987).
[4]M. A. Baldo, D. F. O'Brien, Y. You, A. Shoustikov, S. Sibley, M. E. Thompson, and S. R. Forrest, Nature (London) **395**, 151 (1998).
[5]G. Yu, Y. Cao, J. Wang, J. McElvain, and A. J. Heeger, Synth. Met. **102**, 904 (1999).
[6]P. Peumans, V. Bulovic, and S. R. Forrest, Appl. Phys. Lett. **76**, 3855 (2000).
[7]S. R. Forrest, Nature (London) **428**, 911 (2004).
[8]Z. Chen, B. Cotterell, W. Wang, E. Guenther, and S.-J. Chua, Thin Solid Films **394**, 201 (2001).
[9]Z. Wu, Z. Chen, X. Du, J. M. Logan, J. Sippel, M. Nikolou, K. Kamaras, J. R. Reynolds, D. B. Tanner, A. F. Hebard, and A. G. Rinzler, Science **305**, 1273 (2004).
[10]T. M. Barnes, X. Wu, J. Zhou, A. Duda, J. van de Lagemaat, T. J. Coutts, C. L. Weeks, D. A. Britz, and P. Glatkowski, Appl. Phys. Lett. **90**, 243503 (2007).
[11]M. W. Rowell, M. A. Topinka, M. D. McGehee, H.-J. Prall, G. Dennler, N. S. Sariciftci, L. Hu, and G. Gruner, Appl. Phys. Lett. **88**, 233506 (2006).
[12]M.-G. Kang and L. J. Guo, Adv. Mater. (Weinheim, Ger.) **19**, 1391 (2007).
[13]J.-Y. Lee, S. T. Connor, Y. Cui, and P. Peumans, Nano Lett. **8**, 689 (2008).
[14]K. S. Novoselov, A. K. Geim, S. V. Morozov, D. Jiang, Y. Zhang, S. V. Dubonos, I. V. Grigorieva, and A. A. Firsov, Science **306**, 666 (2004).
[15]S. Watcharotone, D. A. Dikin, S. Stankovich, R. Piner, I. Jung, G. H. B. Dommett, G. Evmenenko, S.-E. Wu, S.-F. Chen, C.-P. Liu, S. T. Nguyen, and R. S. Ruoff, Nano Lett. **7**, 1888 (2007).
[16]C. Gómez-Navarro, R. T. Weitz, A. M. Bittner, M. Scolari, A. Mews, M. Burghard, and K. Kern, Nano Lett. **7**, 3499 (2007).
[17]X. Wang, L. Zhi, and K. Mullen, Nano Lett. **8**, 323 (2008).
[18]E. Rollings, G.-H. Gweon, S. Y. Zhou, B. S. Mun, J. L. McChesney, B. S. Hussain, A. V. Fedorov, P. N. First, W. A. de Heer, and A. Lanzara, J. Phys. Chem. Solids **67**, 2172 (2006).
[19]W. S. Hummers, Jr. and R. E. Offeman, J. Am. Chem. Soc. **80**, 1339 (1958).
[20]M. Hirata, T. Gotou, S. Horiuchi, M. Fujiwara, and M. Ohba, Carbon **42**, 2929 (2004).
[21]H. A. Becerril, J. Mao, Z. Liu, R. M. Stoltenberg, Z. Bao, and Y. Chen, ACS Nano **2**, 463 (2008).
[22]S. R. Forrest, Chem. Rev. (Washington, D.C.) **97**, 1793 (1997).
[23]P. Peumans and S. R. Forrest, Appl. Phys. Lett. **79**, 126 (2001).
[24]J. Xue, S. Uchida, B. P. Rand, and S. R. Forrest, Appl. Phys. Lett. **84**, 3013 (2004).
[25]H. Ago, T. Kugler, F. Cacialli, K. Petritsch, R. H. Friend, W. R. Salaneck, Y. Ono, T. Yamabe, and K. Tanaka, Synth. Met. **103**, 2494 (1999).
[26]P. G. Schroeder, M. W. Nelson, B. A. Parkinson, and R. Schlaff, Surf. Sci. **459**, 349 (2000).
[27]J. Shewchun, J. Dubow, C. W. Wilmsen, R. Singh, D. Burk, and J. F. Wager, J. Appl. Phys. **50**, 2832 (1979).
[28]N. Bakasybramanian and A. Subrahmanyam, J. Electrochem. Soc. **138**, 322 (1991).
[29]F. Nüesch, L. J. Rothberg, E. W. Forsythe, Q. T. Le, and Y. Gao, Appl. Phys. Lett. **74**, 880 (1999).
[30]A. Liu, S. Zhao, S.-B. Rim, J. Wu, M. Konemann, P. Erk, and P. Peumans, Adv. Mater. (Weinheim, Ger.) **20**, 1065 (2008).